Breakup of H_2^+ by one photon in the presence of a strong dc field

Zufar Mulyukov* and Robin Shakeshaft
Physics Department, University of Southern California, Los Angeles, California 90089-0484
(Received 9 August 2000; revised manuscript received 25 September 2000; published 13 April 2001)

We calculate the frequency profile of the rate for breakup of H_2^+ by one photon in the presence of a strong dc field. After photoexcitation of the molecular ion from its ground $1s\sigma$ electronic state to the $2p\sigma$ electronic state, the nuclei are temporarily trapped by a dc field-induced barrier with turning point $R_{\max}$. However, the nuclei are released through either rotation of the internuclear axis (which, for the sake of tractability, we ignore) or dc-field ionization involving resonant transfer from the $2p\sigma$ state to a more highly excited state. The most prominent resonance occurs at an internuclear separation that is less than $R_{\max}$ and, in a.u., is approximately $3/(8F_{\rm dc})+3$, where $F_{\rm dc}$ is the dc field strength. We interpret the change in the frequency profile, as $F_{\rm dc}$ varies, in terms of different aspects of the dynamics of the breakup process, in particular the dispersion of the probability distribution of the nuclei due to over-the-barrier dissociation from the $1s\sigma$ state.

DOI: 10.1103/PhysRevA.63.053404 PACS number(s): 32.60.+i, 33.80.Rv, 33.80.Eh

I. INTRODUCTION

Previous studies of the dissociation and ionization of the one-electron molecular ions H_2^+ and HD^+ by strong ac fields have revealed a wide variety of interesting effects that distinguish the breakup of molecular ions from the breakup of atoms. Among numerous examples we cite bond softening (see, e.g., [1]), vibrational trapping (see, e.g., [2–5]), counterintuitive angular distributions for the fragments emitted in dissociation of HD^+ by a two-color optical field [6], and angular distributions for the fragments emitted in dissociation of HD^+ by a two-color microwave field that depend strongly on which isotope, H^+ or D^+, is released [7]. An informative review of experimental and theoretical aspects of H_2^+ ions in strong laser fields has been given by Giusti-Suzor *et al.* [8].

In the current paper, we present and discuss results of calculations of the frequency profile of the rate for breakup of H_2^+ by one photon in the presence of a strong dc electric field. The photon, supplied by, for example, a moderately weak tunable laser field, can excite the molecular ion from its ground $1s\sigma$ electronic state to the $2p\sigma$ electronic state. The dc field dresses the electronic states in almost the same way as does a low-frequency ac electric field. One-photon dissociation of H_2^+ and HD^+ in the absence of a dressing field was studied experimentally and theoretically some time ago [9,10]. However, the inclusion of a strong dc field radically alters the dynamics, not only by significantly modifying the potential-energy curves along which the nuclei move but also by opening up another pathway for breakup, i.e., ionization.

The exact treatment of a three-body system in an external field is, of course, a formidable challenge, and we are obliged to make a drastic approximation: We restrict the motion of the nuclei to one dimension, along the electric-field axis, with the H_2^+ ion oriented so that prior to excitation its dipole moment is antiparallel to the dc field. As long as the molecular ion remains in the $1s\sigma$ electronic state this orientation is stable. However, if the H_2^+ ion is excited to the $2p\sigma$ state without rotation of the internuclear axis its dipole moment points in the reverse direction, parallel to the dc field, which is an unstable orientation. Therefore the question arises as to whether the rotation of the H_2^+ ion can be ignored during the time it takes for dissociative ionization to occur. It is difficult to give a definitive answer, but we can make a rough assessment as follows: At a moderately large internuclear separation R the dipole moment is $eR/2$ and the frequency of rotation of the dipole in a dc field of strength $F_{\rm dc}$ is $\sqrt{2MR/F_{\rm dc}e}$ where M is the proton mass. The period of rotation must be larger than the time it takes for the H_2^+ ion to separate to the point, $R_{\rm res}$, where resonant ionization leads to rapid breakup. Roughly speaking the latter time is $R_{\rm res}/v$, where $Mv^2/2=\hbar\Omega$ and Ω is the photon frequency. Thus we require $(\hbar\Omega/eF_{\rm dc}R_{\rm res})>1$. In Sec. III we show that $eF_{\rm dc}R_{\rm res}\approx(3/8)$ a.u., and since $\hbar\Omega$ is about 0.7 a.u. our condition is only barely satisfied, if at all. Therefore we do not expect the results of our calculation to provide more than just a qualitative picture. Our remaining approximations are more reliable: We place no restriction on the degrees of freedom of the electron motion. Nor do we place any limit on the number of electronic levels (aside from the limit implicitly imposed by the size of the basis on which the electronic wave function is expanded). While the effect of vibronic coupling, i.e., the explicit coupling of the nuclear and electronic motions, may be expected to be small, we include this coupling since it is not difficult to do so, through leading order in $(m_e/\mu_n)^{1/4}$, where m_e is the electron mass and μ_n is the reduced mass of the nuclei. The error in the wave function incurred within the Born-Oppenheimer approximation is of order $(m_e/\mu_n)^{1/2}$ when the nuclei are frozen and of order $(m_e/\mu_n)^{3/4}$ when the nuclei are allowed to move in the electronic potential generated while the nuclei are frozen [11]. After vibronic coupling is included through leading order, the error in the wave function is only of order (m_e/μ_n). We express the Hamiltonian in terms of the internuclear separation R and *modified* prolate spheroidal electron coordinates,

*Present address: Department of Computer Science and Engineering, University of California, La Jolla, CA 92093-0114.

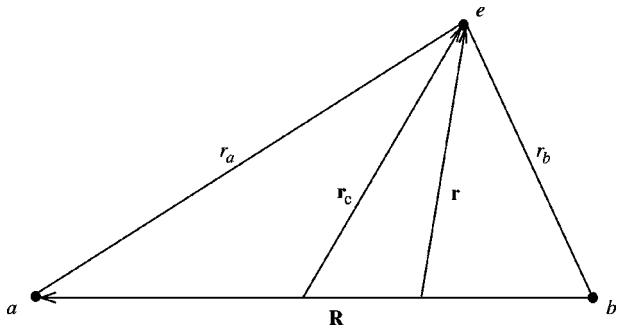

FIG. 1. The coordinate system. The electron e is at distances of r_a and r_b, respectively, from the nuclei a and b, and is located relative to the center of mass of the nuclei, and the midpoint of the nuclei, by $\mathbf{r}$ and $\mathbf{r}_c$, respectively. The vector $\mathbf{R}$ locates a relative to b.

and we expand the complete wave function in terms of basis functions that are tailored to the boundary conditions of the problem. The matrix representing the Hamiltonian is highly sparse when, as done here, vibronic coupling is included only through leading (nonzero) order.

In the next two sections we describe the formalism, beginning with a preliminary discussion in Sec. II and proceeding to the technical details of the calculation in Sec. III. For generality, we do not specify the nuclear masses, and hence our formalism is applicable not just to H_2^+ but to all one-electron molecular ions with nuclei that are isotopes of hydrogen, i.e., HD^+, HT^+, and D_2^+, etc. On several occasions, we pause to note differences that arise between homonuclear and heteronuclear molecular ions. In Sec. IV, we present and discuss our results.

II. PRELIMINARY DISCUSSION

Units in which $\hbar=1$ and the electron charge is -1 are used throughout. The nuclei are labeled by a and b and the electron by e. The masses of a and b are M_a and M_b, their charges are Z_a and Z_b, and the electron mass is m_e. Let $\mathbf{R}$ locate the position of a relative to b, and let $\mathbf{r}$ locate the position of e relative to the center of mass of the nuclei; see Fig. 1. It is convenient to define the following masses and mass ratios:

$$\mu_e = m_e(M_a+M_b)/(m_e+M_a+M_b), \tag{1}$$

$$\mu_n = M_a M_b/(M_a+M_b), \tag{2}$$

$$\alpha = \mu_n/M_a, \tag{3}$$

$$\beta = \mu_n/M_b. \tag{4}$$

If the nuclei are clamped in place, at the separation R, the electronic Hamiltonian is

$$H_e(R) = -\frac{1}{2\mu_e}\boldsymbol{\nabla}_{\mathbf{r}}^2 + \frac{Z_a Z_b}{R} - \frac{Z_a}{|\mathbf{r}-\alpha\mathbf{R}|} - \frac{Z_b}{|\mathbf{r}+\beta\mathbf{R}|}. \tag{5}$$

Allowing the nuclei to move, introducing an external linearly polarized electric field, whose interaction with the molecular ion is $V(t)$, and separating out the motion of the center of mass of the molecular ion, the Hamiltonian governing the internal motion is [12]

$$H(t) = -\frac{1}{2\mu_n}\boldsymbol{\nabla}_{\mathbf{R}}^2 + \frac{Z_a Z_b}{R} + H_e(R) + V(t). \tag{6}$$

Hereafter, corrections of order m_e/μ_n are neglected, and the nuclear charges are restricted to $Z_a=Z_b=1$. Let $\mathbf{F}(t) = F(t)\hat{\mathbf{e}}$ denote the external electric field (which may not depend on the time t), with associated vector potential $\mathbf{A}(t)$. In the length and velocity gauges, respectively, we have

$$V(t) = (\beta-\alpha)\mathbf{F}(t)\cdot\mathbf{R} + \mathbf{F}(t)\cdot\mathbf{r}, \tag{7}$$

$$V(t) = (i/\mu_n)(\beta-\alpha)\mathbf{A}(t)\cdot\boldsymbol{\nabla}_{\mathbf{R}} + (i/m_e)\mathbf{A}(t)\cdot\boldsymbol{\nabla}_{\mathbf{r}}. \tag{8}$$

The terms in $V(t)$ depending on $\mathbf{R}$ and $\mathbf{r}$, respectively, account for the coupling of the nuclear and electronic motions with the external field.

We label the electron states by the united-atom-limit quantum numbers. We assume that in the absence of an external field, the molecular ion is in its ground state; the electron is in the $1s\sigma$ state. If the electron is excited to the $2p\sigma$ state, the molecular ion dissociates. The transformation $\mathbf{R}\rightarrow-\mathbf{R}$ is equivalent to interchanging the nuclei a and b. In the homonuclear case ($M_a=M_b$) we have $\alpha=\beta$ and hence the electronic Hamiltonian $H_e(R)$ is invariant under the interchange of the nuclei. This symmetry implies that the bare homonuclear molecular ion has a twofold degeneracy in its dissociation limit, although this degeneracy is lifted by the external electric field. In the heteronuclear case ($M_a\neq M_b$) we have $\alpha\neq\beta$, and so $H_e(R)$ is no longer invariant under the interchange of the nuclei; the bare heteronuclear molecular ion has two nearly degenerate dissociation limits [13–15]. Assuming that $M_b>M_a$, and recognizing that (due to the reduced mass correction) the system $(b+e)$ has a lower ground-state energy than does $(a+e)$, the lower $(1s\sigma)$ and upper $(2p\sigma)$ dissociation limits of the bare molecular ion $(a+b+e)$ correspond to the asymptotic channels $(b+e)+a$ and $(a+e)+b$, respectively, and these limits are reached along attractive and repulsive potential-energy curves, respectively.

It is instructive to look at the nuclear potential-energy curves for a specific one-electron molecular ion, say HD^+. The deutron is the heavier nucleus b, and $\mathbf{R}$ locates the proton relative to the deutron. In the absence of an external field, the lower and upper dissociation limits, which are split by only 3.7 meV, correspond to the channels in which the electron is bound (in the $1s$ state) to the deutron and proton, respectively. At small to moderate values of the internuclear separation, the probabilities for finding the electron near to the proton and near to the deutron are very nearly equal, no matter whether the electron is in the $1s\sigma$ or $2p\sigma$ state, but as the internuclear separation increases the electron moves towards a particular nucleus. (In contrast, for H_2^+ the probabilities for finding the electron localized near one or another proton remain equal at large internuclear separations.) Now consider what happens when a static electric field $\mathbf{F}_{\rm dc}$

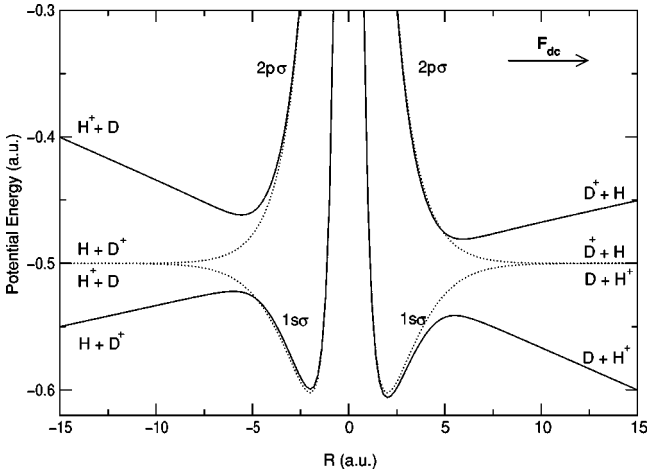

FIG. 2. The $1s\sigma$ and $2p\sigma$ potentials for nuclear motion of HD^+ when dressed by a dc field $\mathbf{F}_{dc}$ of strength 0.01 a.u., with the internuclear line oriented parallel (positive R) or antiparallel (negative R) to $\mathbf{F}_{dc}$. The broken lines are the undressed potential curves; the 3.7-meV separation of the undressed dissociation limits is not visible.

$=F_{dc}\hat{\mathbf{e}}$ is introduced. If, at large internuclear separations, the electron is localized near the deutron (or proton), the dipole moment of the molecular ion relative to the center of mass of the nuclei is $\mathbf{D}=2\mathbf{R}/3$ (or $-\mathbf{R}/3$) since $M_b/M_a=2$. The interaction of this dipole moment with the dc field is $-\mathbf{D}\cdot\mathbf{F}_{dc}$, and for large F_{dc} this interaction strongly distorts the nuclear potentials at large values of R, dwarfing the 3.7 meV separation of the field-free dissociation limits. Figure 2 is a diagram of the dressed and undressed nuclear potential-energy curves, calculated with $\mathbf{R}$ either parallel or antiparallel to $\mathbf{F}_{dc}$; these curves [16] represent the real parts of the $1s\sigma$ and $2p\sigma$ eigenvalues of the Hamiltonian

$$H_{dc}^{(e)}(R)+(\beta-\alpha)\mathbf{F}_{dc}\cdot\mathbf{R}+\frac{1}{R},$$

where $H_{dc}^{(e)}(R)$ is the Hamiltonian of the electron in the presence of the dc field, with the nuclei clamped in place at a fixed value of R, i.e.,

$$H_{dc}^{(e)}(R)=H_e(R)+\mathbf{F}_{dc}\cdot\mathbf{r}. \tag{9}$$

The attractive and repulsive curves, when dressed by the dc field, turn downhill and uphill, respectively, at large R. Thus, in the presence of the dc field the HD^+ ion can dissociate, from its ground state, by tunneling through either the lower left or lower right barrier. While the tunneling rate is very small, the heights of these barriers decrease as the field strength is increased, and when the field is sufficiently strong, over-the-barrier dissociation can occur. The same is true for H_2^+, but in the case of HD^+ the potential-energy curves are asymmetric under the interchange $R\rightarrow -R$. Indeed, since the right barrier is lower and narrower than the left one, the rate for production of H^+ ions is larger than that for D^+ ions.

As indicated in Fig. 2, when $\mathbf{R}$ is antiparallel to $\mathbf{F}_{dc}$ there is a discontinuous interchange of the asymptotic channels once the dc field is turned on. This discontinuity is possible because the dipole coupling energy $F_{dc}R$ is larger than the separation of the field-free dissociation limits for *any* nonzero value of F_{dc} if R is sufficiently large. When $F_{dc}\neq 0$, the electron is forced to move to the nucleus that is consistent with the direction of the molecular dipole moment. Note also that when the nuclei are clamped in place, the undressed electronic wave functions for H_2^+ and HD^+ are the same if these wave functions are expressed in terms of the coordinate $\mathbf{r}_c$ which locates the electron relative to the midpoint of the nuclei. Hence, the field-dressed electronic energy for HD^+ can be obtained from the field-dressed electronic energy for H_2^+ by the change of variables

$$\mathbf{r}=\mathbf{r}_c-(\beta-\alpha)\mathbf{R}/2. \tag{10}$$

This change of variables modifies the term $\mathbf{F}_{dc}\cdot\mathbf{r}$ by $-(\beta-\alpha)\mathbf{F}_{dc}\cdot\mathbf{R}/2$, and when this modification is added to the term $(\beta-\alpha)\mathbf{F}_{dc}\cdot\mathbf{R}$ the difference in the dressed nuclear potentials for H_2^+ and HD^+ is seen to be $(\beta-\alpha)\mathbf{F}_{dc}\cdot\mathbf{R}/2$, i.e., $-\mathbf{F}_{dc}\cdot\mathbf{R}/6$ since $\alpha=\frac{2}{3}$ and $\beta=\frac{1}{3}$.

If the HD^+ ion is electronically excited to the $2p\sigma$ state by a photon, in the presence of the dc field, the molecular ion begins to dissociate but the nuclei become trapped in the upper left or upper right potential well, and it is only by either rotation of the internuclear axis (which we ignore) or dc-field ionization that the molecular ion can break up. As mentioned earlier, a strong dc field acts in almost the same way as a strong low-frequency ac field. However, whereas a dc field gives rise to an infinitely high barrier, an ac field gives rise to a barrier that is of finite height [2–5]. The nuclear potential-energy curves dressed by dc and ac fields differ beyond an internuclear separation that can be estimated as follows: Let $\Delta E_0^{(e)}(R)$ denote the magnitude of the field-free energy splitting between the $1s\sigma$ and $2p\sigma$ electronic energies at an internuclear separation R. In the absence of an external field, the electron is not preferentially localized about either nucleus, at least for small to moderate values of R; the electron oscillates between the nuclei with [17] a characteristic period of $1/\Delta E_0^{(e)}(R)$. If, however, a dc field is included, the electron becomes localized about a particular nucleus, as noted in the preceding paragraph and indicated in Fig. 2. If we were to reverse the direction of $\mathbf{F}_{dc}$, we would have to redraw Fig. 2; the revised curves would be the same as those obtained by rotating the plane of Fig. 2 through 180°. For example, the upper left and right curves on the redrawn Fig. 2 would correspond to the asymptotic channels $H+D^+$ and $D+H^+$, respectively. Consequently, if we were to adiabatically change the direction of $\mathbf{F}_{dc}$, the electron would move from one nucleus to the other. Suppose that instead of a dc field, a monochromatic ac field $\mathbf{F}_{ac}(t)\equiv F_{ac}\sin(\omega t)\hat{\mathbf{e}}$ were introduced. This ac field changes direction every one-half cycle. The change in localization of the electron must take place before the field-free energy splitting $\Delta E_0^{(e)}(R)$ is dwarfed by the dipole coupling energy $F_{ac}\sin(\omega t)R$. Hence the time, say δt, allowed for the electron

to move from one nucleus to the other is given by $F_{\rm ac}\omega R\,\delta t < \Delta E_0^{(e)}(R)$, i.e., $\delta t \approx \Delta E_0^{(e)}(R)/(F_{\rm ac}\omega R)$. However, δt must be larger than the time $1/\Delta E_0^{(e)}(R)$ that it actually takes for the electron to transfer between nuclei. Hence, the nuclear potential-energy curves dressed by an ac field resemble those dressed by a dc field for internuclear separations smaller than a characteristic value of R, which satisfies the equation

$$R=[\Delta E_0^{(e)}(R)]^2/(F_{\rm ac}\omega). \tag{11}$$

Evidently, the solution of this equation increases as ω decreases, but it cannot be large unless ω is very small since $\Delta E_0^{(e)}(R)$ decreases exponentially as R increases.

III. TECHNICAL DETAILS

The electronic Hamiltonian $H_e(R)$ can be simplified by using prolate spheroidal coordinates. To use these coordinates, we must first change variables from $\mathbf{r}$ to $\mathbf{r}_c$. This change leads to a cross term in gradients with respect to $\mathbf{r}_c$ and $\mathbf{R}$ since now differentiation with respect to $\mathbf{R}$ is to be carried out holding $\mathbf{r}_c$, rather than $\mathbf{r}$, constant; see, e.g., [15]. For the purpose of illustration only, a specific gauge, the length gauge, is now adopted; we have, neglecting a term in $(1/\mu_n)\boldsymbol{\nabla}^2_{\mathbf{r}_c}$ (which is of order m_e/μ_n),

$$H(t)=-\frac{1}{2\mu_n}\boldsymbol{\nabla}^2_{\mathbf{R}}-\frac{(\beta-\alpha)}{2\mu_n}\boldsymbol{\nabla}_{\mathbf{R}}\cdot\boldsymbol{\nabla}_{\mathbf{r}_c}+\frac{1}{R}+H_e(R)+\frac{(\beta-\alpha)}{2}\mathbf{F}(t)\cdot\mathbf{R}+\mathbf{F}(t)\cdot\mathbf{r}_c. \tag{12}$$

The separability of $H_e(R)$ in the prolate spheroidal coordinate system (λ,μ,ϕ), with origin at $\mathbf{r}_c=0$, has frequently been exploited. Here, ϕ is the azimuthal angle (with polar axis along the internuclear axis) and

$$\lambda=(r_a+r_b)/R, \tag{13}$$

$$\mu=(r_a-r_b)/R, \tag{14}$$

where $1\leqslant\lambda\leqslant\infty$ and $-1\leqslant\mu\leqslant 1$. We have

$$H_e(R)=\frac{-2}{m_eR^2(\lambda^2-\mu^2)}\left[\frac{\partial}{\partial\lambda}\left((\lambda^2-1)\frac{\partial}{\partial\lambda}\right)+\frac{\partial}{\partial\mu}\times\left((1-\mu^2)\frac{\partial}{\partial\mu}\right)+\left(\frac{1}{(\lambda^2-1)}+\frac{1}{(1-\mu^2)}\right)\frac{\partial^2}{\partial\phi^2}+2m_eR\lambda\right]. \tag{15}$$

Adopting the (drastic) approximation that the internuclear line is oriented along the polarization axis $\hat{\mathbf{e}}$ gives

$$\boldsymbol{\nabla}_{\mathbf{R}}\approx\hat{\mathbf{e}}\frac{\partial}{\partial R}, \tag{16}$$

$$\mathbf{F}(t)\cdot\mathbf{R}=F(t)R, \tag{17}$$

$$\mathbf{F}(t)\cdot\mathbf{r}_c=F(t)(R\lambda/2)\mu. \tag{18}$$

In Eq. (16), differentiation with respect to R is to be carried out holding $\mathbf{r}_c$ constant. However, to use prolate spheroidal coordinates, differentiation with respect to R must be carried out holding λ, μ, and ϕ constant; hence Eq. (16) must be replaced by

$$\boldsymbol{\nabla}_{\mathbf{R}}\approx\hat{\mathbf{e}}\left(\frac{\partial}{\partial R}-\frac{1}{R}\frac{\lambda(\lambda^2-1)}{(\lambda^2-\mu^2)}\frac{\partial}{\partial\lambda}-\frac{1}{R}\frac{\mu(1-\mu^2)}{(\lambda^2-\mu^2)}\frac{\partial}{\partial\mu}\right). \tag{19}$$

In reexpressing $(1/\mu_n)\boldsymbol{\nabla}^2_{\mathbf{R}}$ and $(1/\mu_n)\boldsymbol{\nabla}_{\mathbf{R}}\cdot\boldsymbol{\nabla}_{\mathbf{r}_c}$ in prolate spheroidal coordinates, cross terms involving $\partial/\partial R$ and either $\partial/\partial\lambda$ or $\partial/\partial\mu$ are retained—such cross terms are of the order of the ratio of the momentum of the electron and the relative momentum of the nuclei, i.e., of order $(m_e/\mu_n)^{1/4}$ or higher—but cross terms involving $\partial/\partial\lambda$ and $\partial/\partial\mu$, which are of order (m_e/μ_n), are neglected. Thereby, we arrive at

$$\boldsymbol{\nabla}^2_{\mathbf{R}}\approx\frac{\partial^2}{\partial R^2}-\frac{2}{R(\lambda^2-\mu^2)}\left(\lambda(\lambda^2-1)\frac{\partial}{\partial\lambda}+\mu(1-\mu^2)\frac{\partial}{\partial\mu}\right)\frac{\partial}{\partial R}, \tag{20}$$

$$\boldsymbol{\nabla}_{\mathbf{R}}\cdot\boldsymbol{\nabla}_{\mathbf{r}_c}\approx\frac{2}{R(\lambda^2-\mu^2)}\left((\lambda^2-1)\mu\frac{\partial}{\partial\lambda}+(1-\mu^2)\lambda\frac{\partial}{\partial\mu}\right)\frac{\partial}{\partial R}. \tag{21}$$

When $|\mathbf{r}_c|\gg R$, we have $|\mathbf{r}_c|\approx R\lambda$, but since the asymptotic distance of the electron from the midpoint of the nuclei is of physical importance (it is used to specify the ionization channel boundary condition), it should be expressed in terms of a single independent variable; a suitable variable is

$$\xi\equiv R(\lambda-1), \tag{22}$$

which ranges from 0 to ∞. Therefore, one final change of variables is necessary, i.e., replacement of λ by ξ. Since differentiation with respect to R must now be carried out holding ξ, μ, and ϕ constant, we must make the replacements

$$\frac{\partial}{\partial\lambda}=R\frac{\partial}{\partial\xi}, \tag{23}$$

$$\frac{\partial}{\partial R}\to\frac{\partial}{\partial R}+\frac{\xi}{R}\frac{\partial}{\partial\xi}, \tag{24}$$

$$\frac{\partial^2}{\partial R^2}\to\frac{\partial^2}{\partial R^2}+2\frac{\xi}{R}\frac{\partial}{\partial\xi}\frac{\partial}{\partial R}, \tag{25}$$

where in Eq. (25) we have omitted a term in $\partial^2/\partial\xi^2$, as this is consistent with neglecting terms of order (m_e/μ_n); for the same reason, we can drop the second term on the right side

of Eq. (24). Combining Eqs. (12), (15), and (17)–(25) yields an expression for $H(t)$ in terms of the *entirely independent variables* ξ, μ, ϕ, and R. Taking into account the cylindrical symmetry of the electron motion about $\hat{\mathbf{e}}$, the dependence of $H_e(R)$ on ϕ can be separated out by substitution of $\exp(im\phi)$, where m is the magnetic quantum number of the electron; we assume that the projection of the electron angular momentum along the internuclear axis does not change during the process of alignment of the molecular system along $\hat{\mathbf{e}}$. The final expression for $H(t)$ in terms of ξ, μ, and R is

$$
\begin{aligned}
H(t) = &-\frac{1}{2\mu_n}\left[\frac{\partial^2}{\partial R^2}+2\frac{\xi}{R}\frac{\partial}{\partial\xi}\frac{\partial}{\partial R}\right.\\
&-\frac{2}{R[(\xi+R)^2-(R\mu)^2]}\left(\xi(\xi+R)(\xi+2R)\frac{\partial}{\partial\xi}\right.\\
&\left.\left.+R^2\mu(1-\mu^2)\frac{\partial}{\partial\mu}\right)\frac{\partial}{\partial R}\right]-\frac{1}{\mu_n}\left(\frac{\beta-\alpha}{[(\xi+R)^2-(R\mu)^2]}\right)\\
&\times\left(\xi(\xi+2R)\mu\frac{\partial}{\partial\xi}+(1-\mu^2)(\xi+R)\frac{\partial}{\partial\mu}\right)\frac{\partial}{\partial R}\\
&+H_e(R)+\frac{1}{2}[(\beta-\alpha)R+(R+\xi)\mu]F(t), \qquad (26)
\end{aligned}
$$

where $H_e(R)$ differs from the right side of Eq. (15) only by the change of the variable λ to $\lambda=(\xi+R)/R$, accomplished using Eq. (23), and by the replacement of $\partial^2/\partial\phi^2$ by $-m^2$. Hereafter, since we consider only excitation between σ states, we set $m=0$.

To summarize, the two basic approximations that we have made are (i) the alignment (or antialignment) of the internuclear axis with the polarization axis, and (ii) the inclusion of vibronic coupling only through leading (nonzero) order. Apart from this second approximation, the Hamiltonian of Eq. (26) is exactly equivalent to the Hamiltonian of a molecular ion confined to a rotational level whose angular momentum quantum numbers are zero. From the computational viewpoint, a salient feature of the expression on the right side of Eq. (26) is that it involves only *low-order polynomials* (and derivatives) in ξ, μ, and R, except for the singular factors (discussed again below) $1/R$ and $1/[(\xi+R)^2-(R\mu)^2]$. We represent $H(t)$ on a basis composed of functions of the form

$$u_p(\xi)v_q(\mu)w_s(R),$$

where, with $L_p(x)$ and $P_q(\mu)$ Laguerre and Legendre polynomials, respectively, and with p, q, and s non-negative integers,

$$u_p(\xi)=e^{i\kappa\xi}L_p(-2i\kappa\xi), \qquad (27)$$

$$v_q(\mu)=P_q(\mu), \qquad (28)$$

$$w_s(R)=Re^{iKR}L_s(-2iKR). \qquad (29)$$

Here κ and K lie in the upper right quadrant of the complex plane so that the functions $u_p(\xi)$ and $w_s(R)$ can represent both closed (bound) and open (outgoing-wave) channels. Note the prefactor of R in $w_s(R)$, which conforms with the boundary condition that, once the nuclear motion is restricted to one dimension, the wave function of the molecular system vanishes at $R=0$. The volume element, used in constructing the integral expressions for the matrix elements of $H(t)$, is

$$dV=(\pi/4)[(\xi+R)^2-(R\mu)^2]d\xi\,d\mu\,dR. \qquad (30)$$

The singular factors $1/R$ and $1/[(\xi+R)^2-(R\mu)^2]$, which premultiply derivatives in $H(t)$, disappear in the integrands of the matrix elements since $H(t)$ is premultiplied by $w_s(R)dV$. Noting that $\int_0^\infty dx x^l e^{-x}L_p(x)L_{p'}(x)$ and $\int_{-1}^1 dx x^l P_q(x)P_{q'}(x)$ vanish if $|p-p'|>l$ and $|q-q'|>l$, the matrix representing $H(t)$ on the above basis *is highly sparse*. Consequently, storage requirements, and the number of operations required in manipulating $H(t)$, are minimized.

IV. RESULTS AND DISCUSSION

In this section, we discuss results of calculations of the rate for breakup of H_2^+ by one photon in the presence of a dc field $\mathbf{F}_{dc}=F_{dc}\hat{\mathbf{e}}$ whose axis $\hat{\mathbf{e}}$ is aligned with the polarization axis of the photon. We begin by discussing the dc quasienergy of the electron, denoted by $E_{dc}^{(e)}(R)$; this is a complex eigenvalue of $H_{dc}^{(e)}(R)$, i.e., of the Hamiltonian, defined by Eq. (9), for a molecular ion dressed by a dc field with the nuclei clamped in place. The eigenvalue problem for $E_{dc}^{(e)}(R)$ was solved on a basis composed of the products $u_p(\xi)v_q(\mu)$, where the internuclear separation appears merely as a parameter. The electron energy is shifted at each value of R from its unperturbed value $E_0^{(e)}(R)$ by the amount $\Delta_{dc}^{(e)}(R)$, and it is broadened by the amount $\Gamma_{dc}^{(e)}(R)$. Thus we can write

$$E_{dc}^{(e)}(R)=E_0^{(e)}(R)+\Delta_{dc}^{(e)}(R)-\frac{i}{2}\Gamma_{dc}^{(e)}(R), \qquad (31)$$

with $\Gamma_{dc}^{(e)}(R)$ the rate for ionization from a particular electronic state when the nuclei are at the separation R. Values of $E_{dc}^{(e)}(R)$ have been calculated previously [18,19] for H_2^+ for various values of R and F_{dc}; we have extended these calculations to additional values of R and F_{dc}.

In Fig. 3 we show the $1s\sigma$ and $2p\sigma$ potential-energy curves for the protons when H_2^+ is dressed by a dc field of various strengths. These curves represent the real part of $E_{dc}^{(e)}(R)$ plus the Coulomb repulsion energy, $1/R$, of the protons. We comment below on the solid squares and triangles, which mark the $2p\sigma$ potential curves. Prior to electronic excitation by the photon, the nuclei sit in the lowest vibrational state of the $1s\sigma$ potential well. However, as the dc field increases, the $1s\sigma$ well becomes wider and shallower, and for a dc-field strength above about 0.06 a.u. The molecular ion can dissociate over the barrier to the right of the well. In Fig. 4, we show the probability density for the nuclei to be at a given separation in the initial $1s\sigma$ state, for various

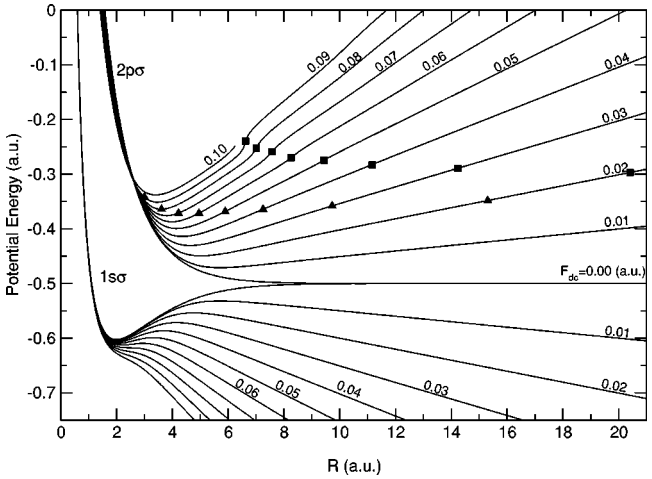

FIG. 3. The $1s\sigma$ and $2p\sigma$ potentials for nuclear motion of H_2^+ when dressed by a dc field of various strengths. We have indicated the internuclear separation at which the rate for ionization from the (dressed) $2p\sigma$ state exhibits its most prominent (solid square) and next most prominent (solid triangle) shape resonance.

dc-field strengths. The ''equilibrium'' separation, say R_0, of the nuclei is the point at which this probability density has its maximum. Note that as the dc-field strength increases, R_0 increases and the probability distribution of the nuclei broadens, corresponding to the change in shape of the $1s\sigma$ potential well.

If the molecular ion is photoexcited to the $2p\sigma$ electronic state, the nuclei become trapped in the $2p\sigma$ potential well, and they would be unable to separate beyond the turning point were it not for either rotation of the internuclear axis (which we ignore) or the existence of a mechanism for rapid transfer of the electron out of the $2p\sigma$ state. In Fig. 5, we show the rate for ionization from the $2p\sigma$ state, i.e., $\Gamma_{\rm dc}^{(e)}(R)$, versus R for various dc-field strengths. Evidently, for each dc-field strength the ionization rate exhibits peaks at several different values of R. These peaks, seen also in earlier calculations [18–20], correspond to resonances.

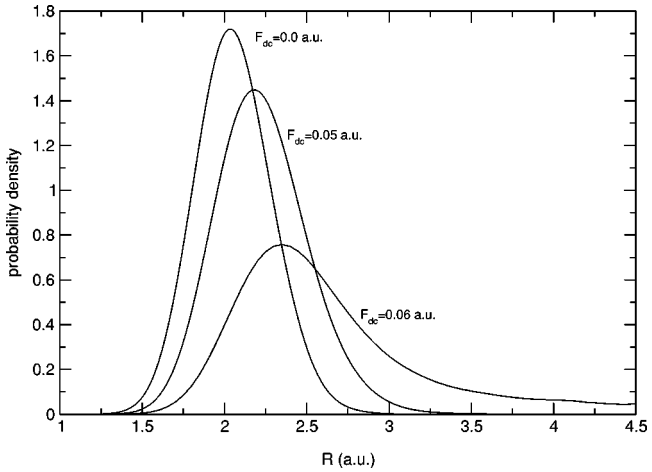

FIG. 4. The normalized probability density for the nuclei to be separated a distance R in the initial $1s\sigma$ state, when dressed by a dc field of various strengths.

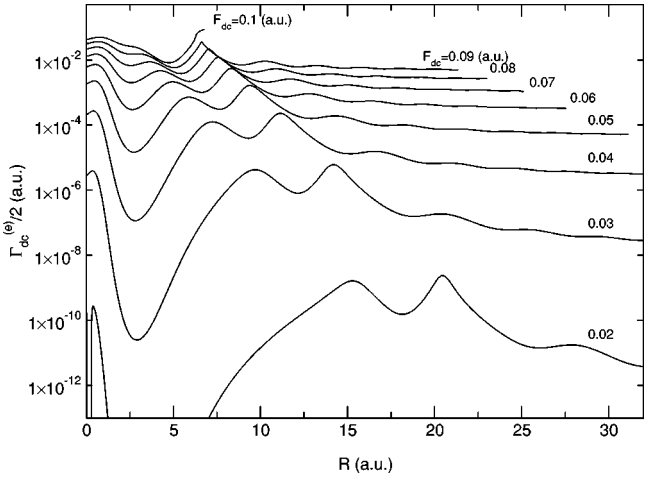

FIG. 5. The half-rate for ionization from the (dressed) $2p\sigma$ state vs internuclear separation R for various dc-field strengths.

The electronic potential, along the direction of $\mathbf{F}_{\rm dc}$—the z axis, say—consists of two wells, each one centered about a different nucleus, with one well higher than the other [21]. In Fig. 6, we show a picture of this potential for particular values of R and $F_{\rm dc}$, i.e., 9 a.u. and 0.0533 a.u., respectively. Plummer and McCann [18] have displayed, most instructively, the electronic potential for a variety of values of R and $F_{\rm dc}$, together with the dressed $1s\sigma$ and $2p\sigma$ electron energy levels. In the absence of the dc field, both wells would have equal heights, and the probabilities for finding the electron localized in one or the other well would be equal, no matter which of the two states—$1s\sigma$ or $2p\sigma$—the electron occupies [17]. However, we see, by referring to Fig. 2, that in the presence of the dc field the localization of the electron (for large R) depends on the electron's state; if the electron is in the $2p\sigma$ state, it is localized about the particular nucleus that gives the molecular system a net dipole moment that points in the direction opposite to that of $\mathbf{F}_{\rm dc}$. Now, the dipole moment of the negatively charged electron

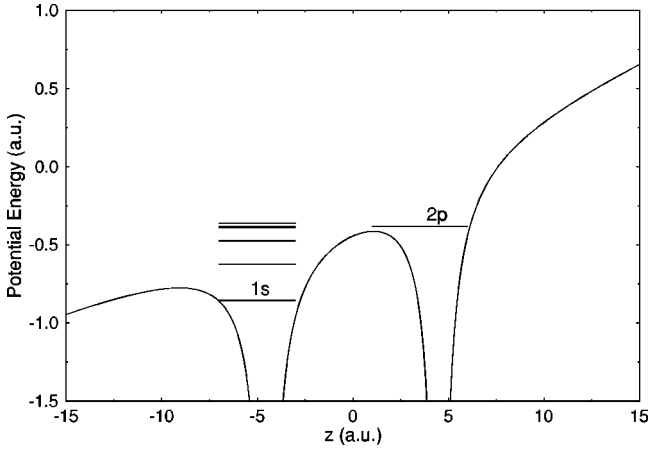

FIG. 6. Electronic potential for H_2^+ along the polarization (z) axis when $R=9$ a.u. and a dc field of strength 0.0533 a.u. is present. We show some of the discrete (autoionizing) levels in the wells.

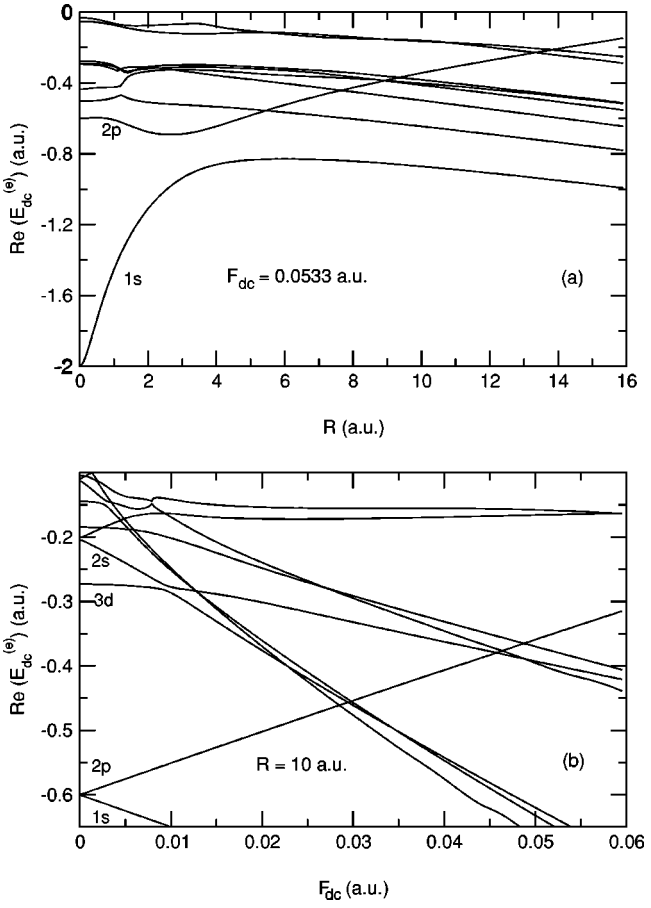

FIG. 7. Real part of the dc quasienergy $E_{\rm dc}^{(e)}(R)$ of the electron for various σ states of H_2^+ (a) vs R when a dc field of strength $F_{\rm dc}=0.0533$ a.u. is present, and (b) versus $F_{\rm dc}$ for $R=10$ a.u.

is $-\mathbf{r}/2$ relative to the midpoint of the nuclei. Hence, when the electron is in the $2p\sigma$ state, it has a dipole moment that is approximately $-(R/2)\hat{\mathbf{e}}$, and the energy arising from the coupling of this dipole to the dc field is $FR/2$. Conversely, when the electron is in the $1s\sigma$ state, the energy arising from the dipole coupling is $-FR/2$. It follows that (for large R) the electron is localized in the upper or lower well according to whether it is in the $2p\sigma$ or $1s\sigma$ state, respectively.

While the $2p\sigma$ energy level shifts upwards as $F_{\rm dc}$ increases, other more highly excited state levels shift downwards, as shown in Fig. 7(b) for $R=10$ a.u. Resonances in the rate for ionization from the $2p\sigma$ state occur at those values of $F_{\rm dc}$ where a highly excited state level crosses the $2p\sigma$ level. The importance of such resonances in enhancing molecular ionization was discussed earlier by Seideman *et al.* [22], who carried out calculations for a model one-dimensional molecular ion exposed to a strong ac field. The crossing points vary with both $F_{\rm dc}$ and R; if $F_{\rm dc}$ is held fixed (but nonzero), crossing points always occur for some values of R. In Fig. 7(a), we show the level crossings for the same value of $F_{\rm dc}$ as was taken in Fig. 6. In Fig. 3, the solid squares and triangles, respectively, mark the internuclear separations at which the rate for ionization from the $2p\sigma$ state exhibits its most prominent and next most prominent resonances. On resonance, the electron can rapidly transfer from the higher well to (a highly excited state in) the lower well of the electronic potential, and the electron can subsequently escape by passing over the outer hump of the lower well. However, it is not necessary for the electron to escape in order for the nuclei to be released; once the electron transfers to the lower well, the nuclei move in a downward-sloping potential, along which they can slide to freedom.

TABLE I. The internuclear separations, $R_{\rm res,1}$ and $R_{\rm res,2}$, at which the two most prominent resonances in the $2p\sigma$ ionization rate occur for different values of the dc-field strength $F_{\rm dc}$. Also shown are the crude estimates, $(3/8F_{\rm dc})\mp 3$, of these resonance positions. All results are in a.u.

$F_{\rm dc}$	$R_{\rm res,1}$	$(3/8F_{\rm dc})-3$	$R_{\rm res,2}$	$(3/8F_{\rm dc})+3$
0.02	15.3	15.7	20.4	21.7
0.04	7.2	6.4	11.2	12.4
0.06	4.9	3.2	8.3	9.2
0.08	3.6	1.7	7.0	7.7

We can make a crude estimate of the internuclear separations at which the two most prominent resonances occur as follows: For large R, and in the absence of the dc field, the energy of the electron in the $2p\sigma$ or $1s\sigma$ state is approximately $-0.5-9/(4R^4)$ in a.u., where the correction of order $1/R^4$ is due to the polarization of the ground-state hydrogen atom, whose polarizability is $\frac{9}{2}$ a.u., by the distant isolated proton. For simplicity, we neglect corrections of order $1/R^4$, and, when the dc field is included, we also neglect corrections of order $F_{\rm dc}^2$ and $F_{\rm dc}/R^2$. Thus the $2p\sigma$ electronic energy, in the presence of the dc field, is

$$E_{2p,\rm dc}^{(e)}(R)\approx -0.5+F_{\rm dc}R/2 \tag{32}$$

in a.u. The levels that shift downwards and cross the $2p\sigma$ level correspond, at asymptotically large R, to channels in which the isolated hydrogen atom is in an excited state. Now, in the presence of a dc field, an excited hydrogen atom has a permanent dipole moment, due to the mixing of degenerate levels with opposite parities, and it therefore undergoes a linear Stark shift. The levels that are closest to the $2p\sigma$ level correspond to asymptotic channels in which the isolated hydrogen atom is in a mixture of $2s$ and $2p$ states, with a Stark shift of $\pm 3F$ in a.u. The energies of these more highly excited levels are therefore

$$E_{\rm ex,dc}^{(e)}(R)\approx -0.125-F_{\rm dc}R/2\pm 3F_{\rm dc} \tag{33}$$

in a.u. The resonances occur where $E_{\rm ex,dc}^{(e)}(R)=E_{2p,\rm dc}^{(e)}(R)$, i.e., where, in a.u.,

$$R\approx (3/8F_{\rm dc})\pm 3. \tag{34}$$

According to this rather crude estimate, the two most prominent resonances occur at internuclear separations that (i) decrease as $F_{\rm dc}$ increases and (ii) differ by 6 a.u. We can assess the validity of Eq. (34) by perusal of Fig. 3 and Table I; not surprisingly, our estimates of the resonance positions are more accurate at smaller field strengths, i.e., at larger R. The most prominent of the two resonances is the one occurring at

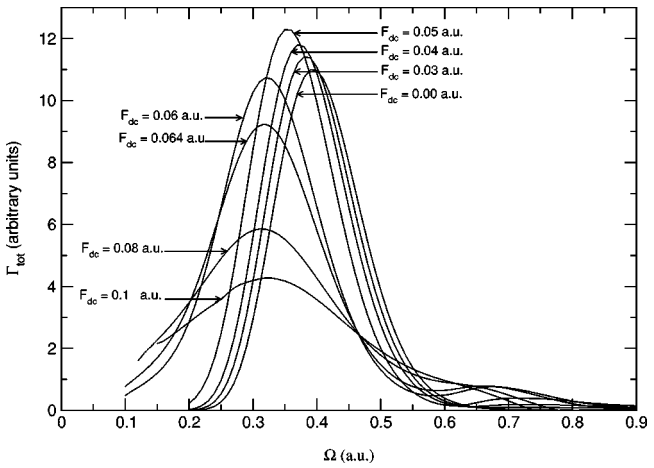

FIG. 8. The frequency profile of the total breakup rate for H_2^+ for various dc-field strengths.

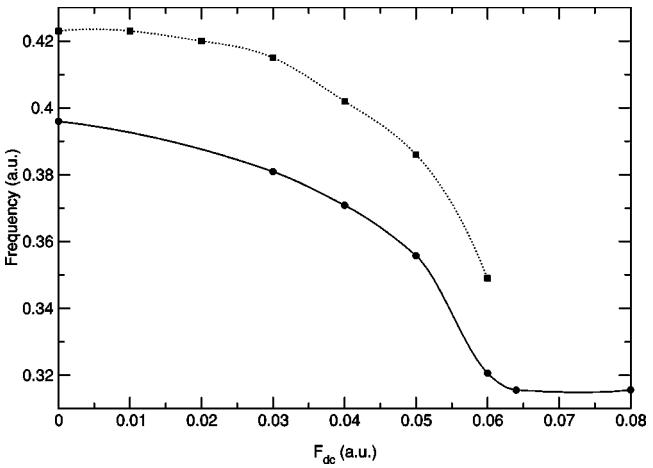

FIG. 9. The frequency at which the profile of the breakup rate has its maximum, for various dc-field strengths. The dashed line is the energy splitting, Ω_0, of the dressed $1s\sigma$ and $2p\sigma$ electronic energies at the ''equilibrium'' separation R_0.

the larger internuclear separation, i.e., close to $(3/8F_{\rm dc})+3$ a.u., since the outer hump of the lower well of the electronic potential, over which the electron must pass if it is to escape, becomes narrower as R increases, and the likelihood of the electron backscattering from this hump diminishes.

To obtain the dc quasienergy, $E_{\rm dc}$, of the molecular ion we solved the eigenvalue problem

$$H_{\rm dc}|\Phi_{\rm dc}\rangle = E_{\rm dc}|\Phi_{\rm dc}\rangle, \tag{35}$$

where $H_{\rm dc}$ is the Hamiltonian of the complete molecular ion dressed by the dc field; we took $H_{\rm dc}$ to be the right side of Eq. (26) with $F(t)$ replaced by $F_{\rm dc}$. The eigenfunction $\Phi_{\rm dc}(\xi,\mu,R)$ is a linear combination of the products $u_p(\xi)v_q(\mu)w_s(R)$, where $u_p(\xi)$, $v_q(\mu)$, and $w_s(R)$ were defined [23] by Eqs. (27)–(29). The probability density for the nuclei to be at the separation R is

$$(\pi/4)\int_0^\infty d\xi \int_{-1}^{1} d\mu[(\xi+R)^2-(R\mu)^2]|\Phi_{\rm dc}(\xi,\mu,R)|^2.$$

This is the density shown in Fig. 4 for the $1s\sigma$ state. The rate at which the molecular ion breaks up due to a dc field is $\Gamma_{1s,\rm dc} = -2\,{\rm Im}\,E_{1s,\rm dc}$, where the label $1s$ has been added as a reminder that the initial state is the ground state. When a moderately weak monochromatic ac field $\mathbf{F}_{\rm ac}(t) \equiv F_{\rm ac}\cos(\Omega t)\hat{\mathbf{e}}$ is also included, the total rate for breakup by one photon in the presence of the dc field is, treating the ac field as a perturbation,

$$\Gamma_{1s,\rm tot} = \Gamma_{1s,\rm dc} + \Gamma_{1s,\rm ac}, \tag{36}$$

where $\Gamma_{1s,\rm ac}$ is the contribution due to the ac field:

$$\Gamma_{1s,\rm ac} = -2\,{\rm Im}\langle\Phi_{1s,\rm dc}|V_- G_{\rm dc}(E_{1s,\rm dc}+\Omega)V_+|\Phi_{1s,\rm dc}\rangle, \tag{37}$$

where $G_{\rm dc}(E) = 1/(E-H_{\rm dc})$ and where, adopting the length gauge,

$$V_\pm = F_{\rm ac}\hat{\mathbf{e}}\cdot\mathbf{r}/2. \tag{38}$$

In Fig. 8 we show the frequency profile of $\Gamma_{1s,\rm tot}$ for various dc-field strengths. The small hump on the high-frequency side of this profile is due to electronic transitions to σ states that are more highly excited than the $2p\sigma$ state.

As $F_{\rm dc}$ increases, the frequency profile shifts to lower frequencies, at least until $F_{\rm dc}$ reaches the strength, about 0.06 a.u., at which over-the-barrier dissociation from the $1s\sigma$ well becomes possible. This is clear from Fig. 9, where we show the frequency at which the peak in the profile occurs versus $F_{\rm dc}$. The shift in the profile as $F_{\rm dc}$ varies below the threshold for over-the-barrier dissociation can be understood from the condition for the $1s\sigma \rightarrow 2p\sigma$ electronic transition to be on

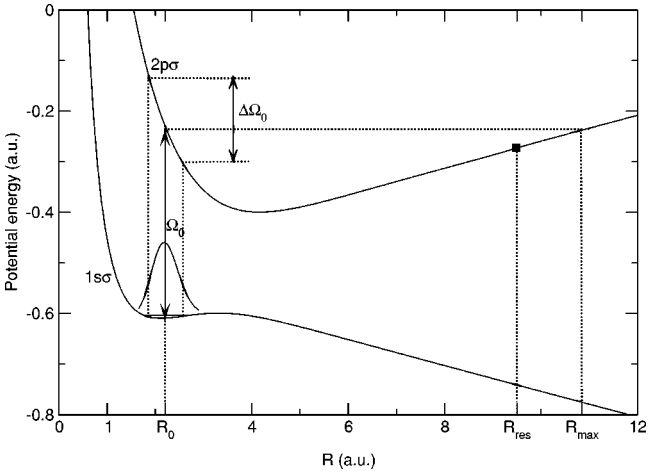

FIG. 10. Schematic diagram showing resonant electronic excitation from the $1s\sigma$ state to the $2p\sigma$ state by a photon of frequency Ω_0 in the presence of a dc field. Here R_0 is the ''equilibrium'' separation of the nuclei in the initial (dressed) $1s\sigma$ state, $R_{\rm max}$ is the maximum separation to which the nuclei can dissociate after photoexcitation, and $R_{\rm res}$ is the internuclear separation at which the rate for ionization from the $2p\sigma$ state exhibits its most prominent resonance. The width of the frequency profile, when determined from the condition for resonant excitation, is $\Delta\Omega_0$.

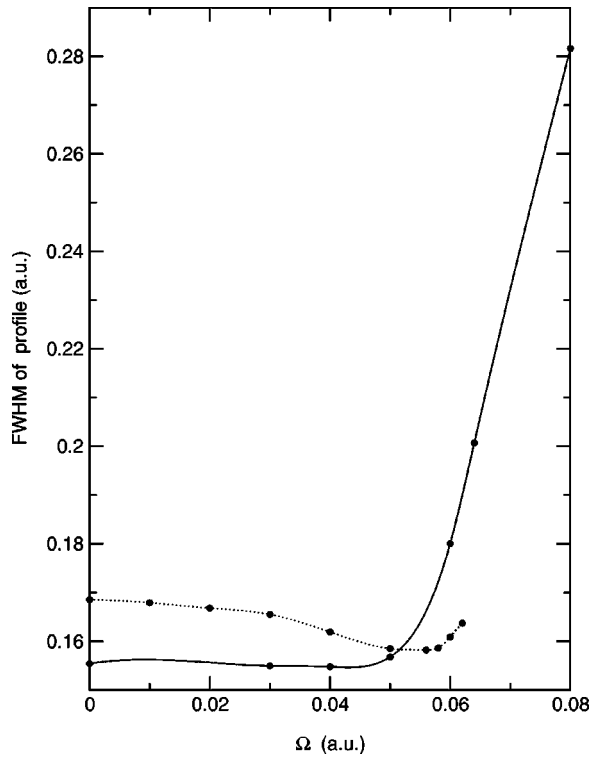

FIG. 11. The full width at half maximum of the frequency profile, for various dc-field strengths. The dashed line is the width $\Delta\Omega_0$ (determined from the condition for resonant excitation)—see Fig. 10.

resonance. This condition—see Fig. 10—is that $\Omega=\Omega_0$, where Ω_0 is the energy splitting of the dressed $1s\sigma$ and $2p\sigma$ electronic energies at R_0, the ''equilibrium'' (i.e., most probable) separation of the nuclei. We show Ω_0 in Fig. 9. While Ω_0 overestimates the frequency at which the profile has its peak [24], the trend in Ω_0 as $F_{\rm dc}$ increases is consistent with the shift in the profile (below the threshold for over-the-barrier dissociation).

The width of the frequency profile remains almost constant, decreasing slightly, as $F_{\rm dc}$ increases, until $F_{\rm dc}$ reaches about 0.05 a.u. This is clear from Fig. 11. The contribution to the width of the profile from the dc width of the $1s\sigma$ energy level is negligible over the range of field strengths considered. Rather, the width of the profile is related, primarily, to the width of the probability distribution of the nuclei. The variation in Ω_0 that is allowed by the resonance condition is shown as $\Delta\Omega_0$ in Fig. 10. Just as Ω_0 overestimates the frequency at which the profile has its peak, so does $\Delta\Omega_0$ overestimate the width of the profile [24], but the trend is again consistent. However, the absence of broadening of the frequency profile for $F_{\rm dc}<0.05$ a.u. is perhaps surprising since it is evident from Fig. 4 that the probability distribution of the nuclei does broaden significantly as $F_{\rm dc}$ increases. It turns out, fortuitously, that the shift in R_0 is such that $\Delta\Omega_0$ hardly changes. The broadening of the frequency profile for $F_{\rm dc}>0.05$ a.u. is due primarily to the merging of the main part of the profile with the hump on the high-frequency side, reflecting the increasing importance of electronic transitions to σ states that are more highly excited than the $2p\sigma$ state.

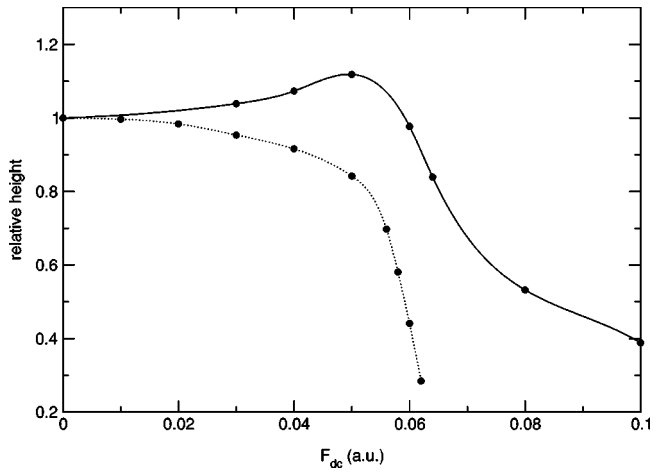

FIG. 12. The relative height of the frequency profile, for various dc-field strengths. The dashed line is the relative height of the initial probability distribution of the nuclei with respect to their separation in the $1s\sigma$ potential well; this probability distribution has been renormalized so that it is equal to the height of the frequency profile when $F_{\rm dc}=0$.

The height of the profile at first increases slightly as $F_{\rm dc}$ increases, and then decreases rapidly. This is clear from Fig. 12. We believe that the initial slight increase in the profile's height is due to the shift to lower frequencies (recall Fig. 9), which results in a larger oscillator strength for the electronic $1s\sigma$-$2p\sigma$ excitation. To explain the sharp falloff in the profile's height when $F_{\rm dc}$ increases beyond about 0.05 a.u., we refer again to Fig. 12, where we show also the relative height of the initial probability distribution of the nuclei in the $1s\sigma$ potential well. The height of this probability distribution decreases immediately as $F_{\rm dc}$ increases (due to the broadening of the distribution) and the effect is to reduce the oscillator strength for photoexcitation. At first, the decrease in the height of the probability distribution of the nuclei is gentle, and is more than compensated for by the shift to lower fre-

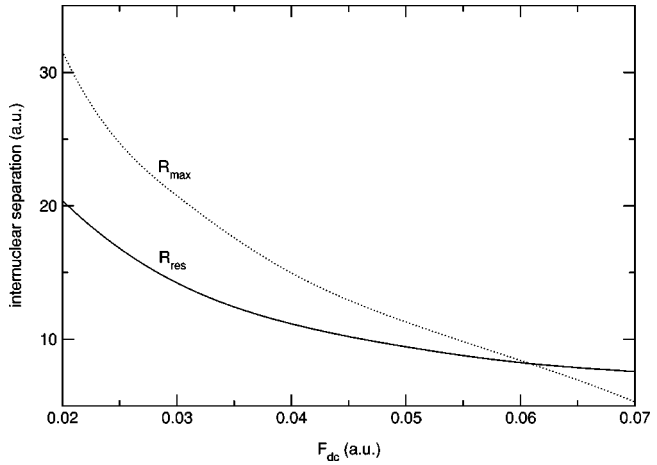

FIG. 13. The internuclear separation, $R_{\rm res}$, at which the rate for ionization from the $2p\sigma$ state exhibits its most prominent resonance. The dashed line is the maximum separation, $R_{\rm max}$, to which the nuclei can dissociate after photoexcitation.

quencies, but as F_{dc} approaches the threshold for over-the-barrier dissociation, the dispersion of the nuclei becomes severe, and dominates at $F_{dc} \approx 0.05$ a.u.

We have ignored the rotation of the H_2^+ ion, and, to the extent that this is legitimate, dissociation is impeded by the field-induced barrier, which opposes the movement of the nuclei beyond the turning point, R_{max} say. In order for the nuclei to separate beyond R_{max} it is necessary that the most prominent resonance occur at an internuclear separation, R_{res} say, which is less than R_{max}. The closer R_{res} is to R_{max}, while remaining less than R_{max}, the longer the time the resonance exerts its influence since the nuclei slow down as they approach the field-induced barrier. In Fig. 13 we show R_{max} and R_{res} vs F_{dc}. We see that R_{max} approaches, but remains above, R_{res} until F_{dc} reaches about 0.06 a.u., at which point over-the-barrier dissociation from the initial state begins to play an important role.

ACKNOWLEDGMENTS

We thank Dr. Bernard Piraux for his helpful contributions in the early stage of this project. This work was supported by the NSF under Grant No. PHY-0070936.

[1] P. H. Bucksbaum, A. Zavriyev, H. G. Muller, and D. W. Schumacher, Phys. Rev. Lett. **64**, 1883 (1990).
[2] G. Yao and S. -I. Chu, Chem. Phys. Lett. **197**, 413 (1992).
[3] A. Giusti-Suzor and F. Mies, Phys. Rev. Lett. **68**, 3869 (1992).
[4] E. E. Aubanel, J. M. Gauthier, and A. D. Bandrauk, Phys. Rev. A **48**, 2145 (1993).
[5] O. Atabek, M. Chrysos, and R. Lefebvre, Phys. Rev. A **49**, R8 (1994).
[6] B. Sheehy, B. Walker, and L. F. DiMauro, Phys. Rev. Lett. **74**, 4799 (1995).
[7] E. Charron, A. Giusti-Suzor, and F. Mies, Phys. Rev. Lett. **75**, 2815 (1995).
[8] A. Giusti-Suzor, F. H. Mies, L. F. DiMauro, E. Charron, and B. Yang, J. Phys. B **28**, 309 (1995).
[9] N. P. F. B. Van Asselt, J. G. Maas, and J. Los, Chem. Phys. **11**, 253 (1975).
[10] J. B. Ozenne, J. Durup, R. W. Odom, C. Pernot, A. Tabaché-Fouhaillé, and M. Tadjeddine, Chem. Phys. **16**, 75 (1976).
[11] L. D. Landau and E. M. Lifshitz, *Quantum Mechanics*, 3rd ed. (Pergamon, New York, 1975)
[12] J. R. Hiskes, Phys. Rev. **122**, 1207 (1961).
[13] A. Dalgarno and R. McCarroll, Proc. R. Soc. London, Ser. A **237**, 383 (1956).
[14] S. Cohen, D. L. Judd, and R. J. Riddell, Jr., Phys. Rev. **119**, 384 (1960).
[15] A. Carrington, I. R. McNab, and C. A. Montgomerie, J. Phys. B **22**, 3551 (1989).
[16] Note that the potentials drawn in the present Fig. 2 differ qualitatively from those drawn by Hiskes [12] in his Fig. 6; the curves drawn by Hiskes cross when **R** is antiparallel to **F**. This discrepancy might be due to the trial wave functions used by Hiskes, which might produce preferential localization of the electron about one or the other nucleus that is erroneous at small values of *R*.
[17] See, e.g., J. C. Slater, *Quantum Theory of Molecules and Solids* (McGraw-Hill, New York, 1963), Vol. 1.
[18] M. Plummer and J. F. McCann, J. Phys. B **29**, 4625 (1996).
[19] Z. Mulyukov, M. Pont, and R. Shakeshaft, Phys. Rev. A **54**, 4299 (1996).
[20] T. Zuo and A. D. Bandrauk, Phys. Rev. A **52**, R2511 (1995).
[21] K. Codling, L. J. Frasinski, and P. A. Hatherly, J. Phys. B **22**, L321 (1989).
[22] T. Seideman, M. Yu. Ivanov, and P. B. Corkum, Phys. Rev. Lett. **75**, 2819 (1995).
[23] Typical values of the wave numbers κ and K of the basis functions $u_p(\xi)$ and $w_s(R)$, respectively, were $|\kappa| = 0.5$ a.u., $|K| = 10.0$ a.u., $\arg(\kappa) = 20°$, and $\arg(K) = 10°$. For a typical basis, the indices p, q, and s of $u_p(\xi)$, $v_q(\mu)$, and $w_s(R)$ were in the ranges $0 \leqslant p \leqslant 15$, $0 \leqslant q \leqslant 15$, and $0 \leqslant s \leqslant 50$.
[24] The oscillator strength of the electronic transition is larger on the lower-frequency side of the profile, so this side should be more heavily weighted.